9ICEG

Evaluation on hydraulic conductivity of saturated bentonites containing different exchangeable cation composition

D. Ito[1], H. Wang[2] and H. Komine[3]

[1]*Assistant professor, Waseda University, Tokyo, Japan, email: daichi_ito@aoni.waseda.jp*

[2]*Associate professor, Waseda University, Tokyo, Japan, email: whlxy2002@aoni.waseda.jp*

[3]*Professor, Waseda University, Tokyo, Japan, email: hkomine@waseda.jp*

ABSTRACT

Barrier materials with low permeability are required for disposal facilities of radioactive wastes, therefore, bentonites are planned to be used. The required permeability varies depending on the radioactivity of wastes, so various bentonites are being considered. In Japan, for high-level radioactive waste (HLW) disposal, Na−bentonite which has low permeability, will be used. While for low-level radioactive waste (LLW) disposal, Ca-bentonite which has relative higher permeability than Na-bentonite in same dry density, can be used. Because HLW disposal project will take several decades to complete, it is necessary to consider a wide range of optional bentonites. In this study, a Mg-Ca bentonite (MG), in which Mg^{2+} and Ca^{2+} between montmorillonite layers are dominant, a Na-bentonite (K_V1) and a Ca-bentonite (KB) was studied and compared in terms of their hydraulic conductivity k. A newly developed test system with specimen thickness of 2 mm was used for obtaining k, by which results can be obtained in a few days, much shorter than conventional test systems. The results showed that k of all bentonites tended to decrease as dry density increased. The effective montmorillonite density ρ_{em}, calculated by dividing the dry mass of montmorillonite by the volume of montmorillonite and pore, was used as a parameter to compare among tested bentonites. The k of MG and KB was 2 to 10 times higher than that of K_V1 in terms of ρ_{em} in the range of 0.8~1.2 Mg/m³. The k of KB and MG were found to be almost the same under the same ρ_{em}.

Keywords: Bentonite, Hydraulic conductivity, Exchangeable cation, Radioactive waste disposal

1   BACKGROUND

Bentonite materials have low permeability and are planned to be used in disposal facilities of various radioactive wastes (Pusch, 1992; Sellin & Leupin, 2013.). The required isolation time differs depending on the level of radioactive waste, and several types of bentonites may be used as the barrier layer. In addition, because geological disposal and other disposal projects are expected to last for several decades in worldwide, future material availability and quality instability will affect the disposal projects (NUMO, 2022.). Based on the above, Mg-Ca bentonite was selected as the target material in this study, in addition to Na- and Ca-bentonite, which have been mainly used in studies on geological disposal and low-level radioactive waste disposal in Japan (Komine & Ogata, 1994; Wang et al., 2022a; Kobayashi et al., 2017.). The hydraulic conductivity of the bentonites was measured using a newly developed permeability test apparatus with a 2-mm-thick specimen, and the effect of exchangeable cations of the bentonites on the hydraulic conductivity was discussed.

2   SAMPLE AND TESTING METHOD

2.1   Bentonite samples used in this study

Three types of Japanese bentonites were used in this study. Kunigel V1 (K_V1) was mined from Tsukinuno Mine in Yamagata and has been widely studied as a buffer material for geological disposal in Japan. Kunibond (KB), mined from Dobuyama Mine in Miyagi, has been studied in research on low-level radioactive waste disposal. Mikawa Raw Ore (MG), mined from Mikawa Mine in Niigata, has not

been researched as a candidate material for radioactive waste disposals, however, this is a relatively rare bentonite material that contains Mg^{2+} ions as the major exchangeable cation and is likely to be the subject of further research (NUMO, 2022.). The basic properties of these three types of bentonites are shown in Table 1. Also, appearance of these bentonites is shown in Figure 1. The montmorillonite content of K_V1 is 52.8%, KB 71.1%, and MG 48.7%, as determined by methylene blue adsorption tests. Based on the leaching cation measurements, the predominant exchangeable cations were Na^+ for K_V1, Ca^{2+} for KB, and Ca^{2+} and MG^{2+} for MG. Leached cations were measured using benzyl-trimethyl ammonium chloride (SFSA method), which has low solubility in associated minerals such as calcium carbonate (Shirakawabe et al., 2022.). Therefore, in the theoretical evaluation equation for hydraulic conductivity described in chapter 3, the obtained leached cation amount is assumed to be the same as the exchangeable cations in montmorillonite.

***Table 1.*** *Basic properties of bentonites used in this study.*

Bentonite name	Soil particle density (Mg/m^3)	Liquid limit (%)	Plastic limit (%)	Content of montmorillonite (%)	Leached Na^+ cation (cmol/kg)	Leached Ca^{2+} cation (cmol/kg)	Leached Mg^{2+} cation (cmol/kg)	Leached K^+ cation (cmol/kg)
K_V1	2.76	535.4	26.7	52.8	53.8	35.5	4.1	1.6
KB	2.53	118.0	45.9	71.1	8.3	61.8	15.3	0.2
MG	2.53	99.0	35.3	48.7	8.1	22.7	21.2	1.2

Figure 1. *Appearance of bentonites used in this study (Left: K_V1, Middle: KB, Right: MG).*

2.2   Hydraulic conductivity test system

Hydraulic conductivity tests system in this study was portrayed in Figure 1 (Ito et al., 2022.). This system consists of a test cell, two burettes, and two pressure regulators. Burettes with a minimum scale of 0.1 mL and capacity of 10 mL were used for water inflow and outflow measurements. The burettes were installed in acrylic pipes, by which water pressure in burettes can be adjusted through pressure regulators. Polyolefin tubes with 2 mm inner diameter were used to connect burettes and the testing cell reducing water evaporation. Membrane filters made of polyether sulfone with 0.45 μm pore size and 140 μm thickness (Nishimura et al., 2011) were placed at the top and bottom surfaces of the specimen. The value of k of the filter was measured as 2.0×10^{-8} m/s.
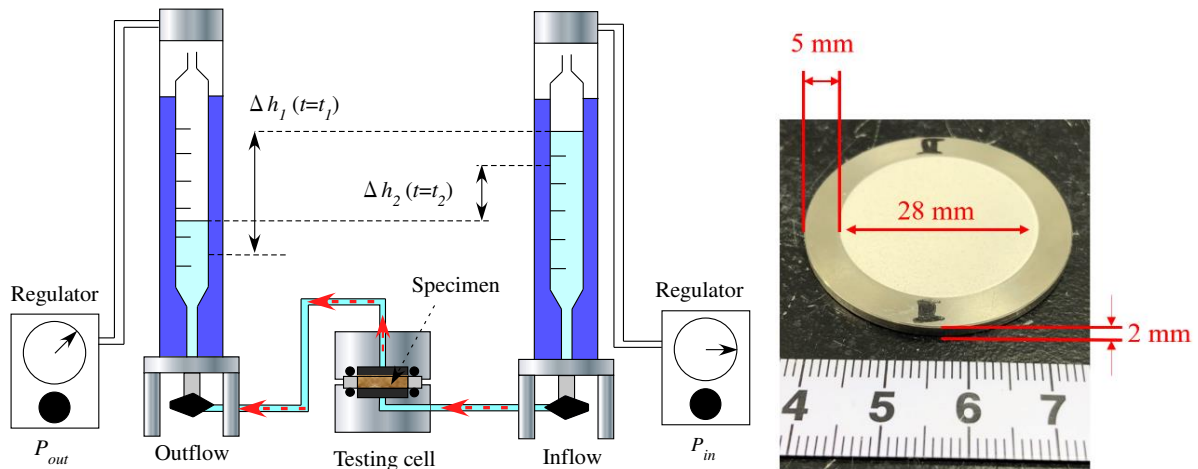
Figure 2. *Hydraulic conductivity test system (Left: Overview of whole system, Right: Specimen view)*

Table 2. *List of test conditions conducted in this study.*

Bentonite name	Specimen Number	Specimen dry density (Mg/m³)	Initial water content (%)	Approximate hydraulic gradient (-)
K_V1	K_V1-1	1.19	7.0	4000
	K_V1-2	1.36	7.0	8000
	K_V1-3	1.61	7.0	10000
	K_V1-4	1.79	9.1	4000→8000→12000→16000
	K_V1-5	1.90	8.4	4000→12000→20000→25000
KB	KB-1	1.09	15.5	1000
	KB-2	1.16	15.5	1000
	KB-3	1.26	17.8	1000→2000
	KB-4	1.32	15.5	1000
	KB-5	1.40	17.8	2000→3000→4000
MG	MG-1	1.15	7.0	1000
	MG-2	1.29	7.0	2000
	MG-3	1.36	7.0	1000
	MG-4	1.47	7.0	1000→2000→3000
	MG-5	1.57	7.0	2000→4500

Specimens of 28 mm diameter and 2 mm height for the three types of bentonites were used in the experiments by compaction to initial dry densities in the range of 1.19 to 1.90 Mg/m³ for K_V1, 1.09 to 1.40 Mg/m³ for KB, and 1.15 to 1.57 Mg/m³ for MG, respectively. To prepare a specimen, a predetermined amount of each bentonite powder in the range of 1.4~2.5 g was compacted into the specimen ring directly. The specimen weight was found using a balance up to 1 mg. Also, the thickness and diameter were measured to the nearest 1 mm during specimen preparation. The specimen dry density was calculated based on the obtained mass, dimensions, and initial water content. The initial water content before compaction was the natural water content of each sample without any addition of water. Table 2 shows test conditions conducted in this study.

After the specimen was assembled into the testing cell, the cell was immersed in distilled water for a day with decompression to approximately -98 kPa for specimen saturation. A saturation confirmation test was conducted by changing the soaking time, and it was confirmed that the specimens were sufficiently saturated after one day of reduced-pressure water supply. Then the cell was connected to the burettes, carefully ensuring that no air was tramped along the water flow path. Finally, air pressure was applied to two burettes gradually. In some cases, the applied pressures were changed to several stages for some specimens to change hydraulic gradient i. In this paper, quite high i of 1000-25000 were applied to shorten the test period. Additionally, applied pressures were kept to less than the swelling pressures of test specimens, referring to measurements results of 2-mm thick compacted bentonite specimens by Wang et al. (2022b) to prevent deformation. The room temperature and water levels of the burettes were recorded with arbitrary time intervals.

The value of k at the testing temperature (k_T) was calculated using Equation (1) and was converted to a value at 15°C (k_{15}) with Equation (2) based on JGS (2018).

$$k_T = 2.303(A_{in} \times A_{out})L/\{(A_{in} + A_{out})A_{spe}(t_2 - t_1)\}\log_{10}(\Delta h_1 \gamma_w + \Delta P)/(\Delta h_2 \gamma_w + \Delta P) \quad (1)$$

$$k_{15} = k_T \times \eta_T/\eta_{15} \quad (2)$$

In those equations, the following variables are used: A_{in} and A_{out} respectively stand for the cross-sectional areas of the burette on both inflow and outflow side (=0.51 cm²); L denotes the specimen thickness; A_{spe} expresses the cross-sectional area of the specimen; Δh_1 and Δh_2 respectively signify the water level differences at times t_1 and t_2; γ_w represents the unit volume weight of water; ΔP represents the differential pressure between the inflow (P_{in}) and outflow (P_{out}); and η_T/η_{15} is the correction factor for calculating k_{15}.

3   RESULTS AND DISCUSSIONS

Figure 3 shows the time course of inflow and outflow volume of each bentonite, which two representative cases are shown, respectively. The inflow and outflow volume on the vertical axis are divided by the initial pore volume of each specimen. The results show that in all cases, a flow volume equivalent to the initial pore volume was obtained in approximately 10 to 15 days. Also, in both cases, the inflow and outflow volume were well balanced throughout the test period, indicating that the flow was steady.
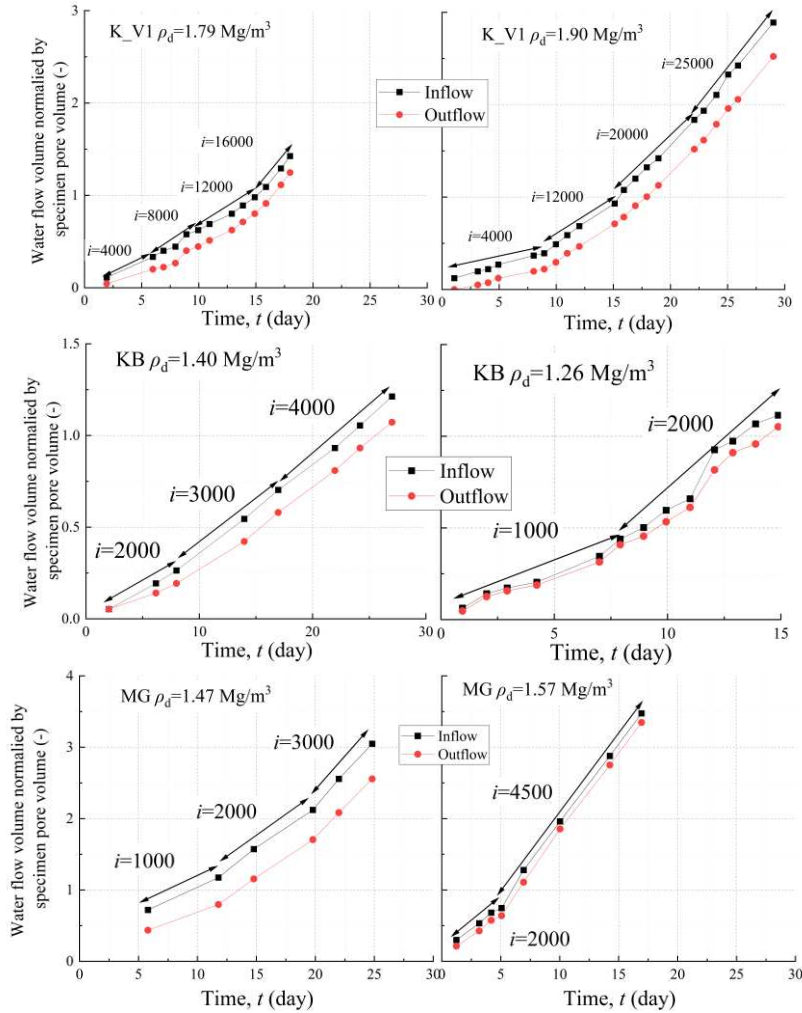
**Figure 3.** *Time course of water flow volume of each bentonite.*
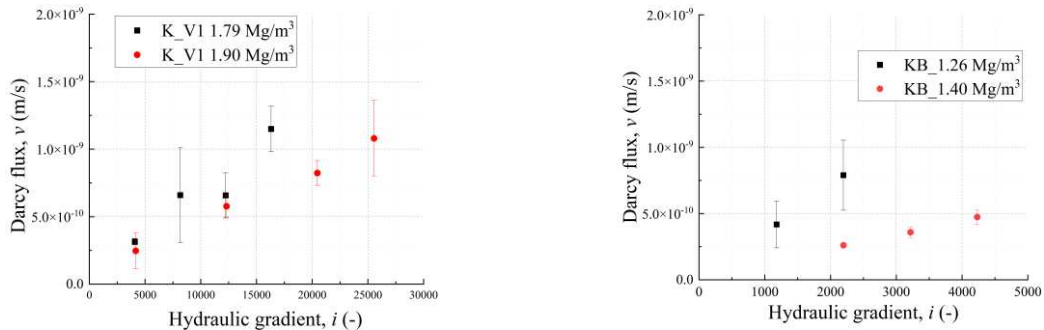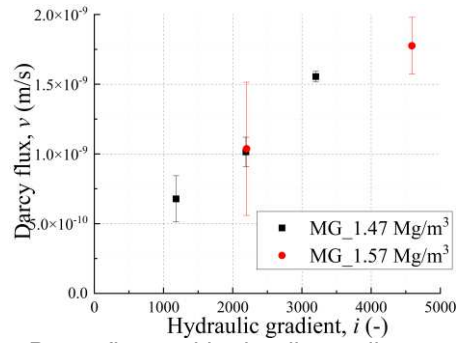
Figure 4. *Relationship between Darcy flux and hydraulic gradient.*

Figure 4 shows the relationship between Darcy flux and hydraulic gradient. In these figures, only the cases where the hydraulic gradient was varied during the test period are shown (K_V1-4, K_V1-5, KB-3, KB-5, MG-4, MG-5). Although there is some variation in some cases, it is generally within a factor of two. The proportional relationship between Darcy flux and hydraulic gradient indicates that Darcy's law is valid for the range of hydraulic gradient applied in this study.

Figure 5 shows the relationship between hydraulic conductivity and dry density for each bentonite. Data from previous studies that measured the hydraulic conductivity of the same bentonite using falling head test and high-pressure consolidation test are also included (Matsumoto et al., 1997; Hasegawa, 2004; Butsuda et al., 2006; NUMO, 2022.) The logarithm of the hydraulic conductivity decreases linearly with increasing dry density for all bentonites. The permeability values obtained in this study are reasonable because they are of the same order and have the same trend as the data obtained in the literature.


(a)

(b)

(c)
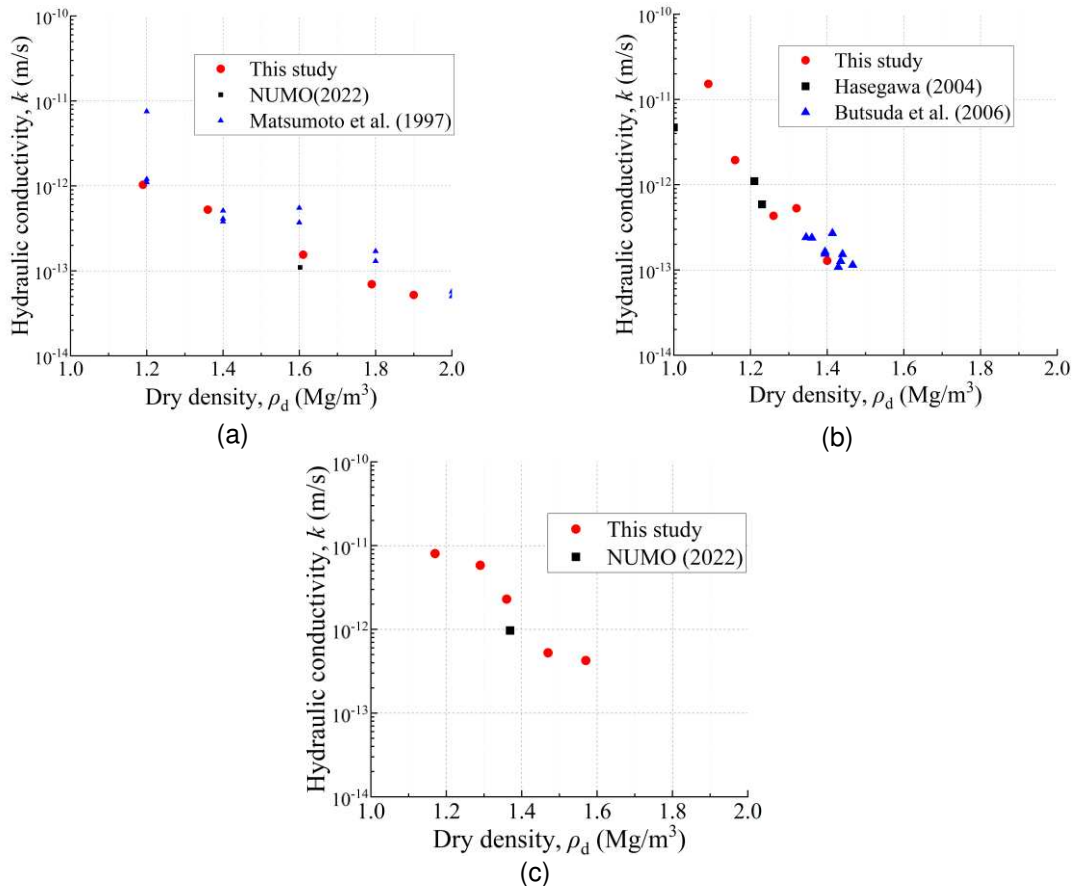
Figure 5. *Relation between hydraulic conductivity and dry density in each bentonties, (a) K_V1, (b) KB, and (c) MG.*

Previous study has shown that the permeability of bentonite depends on the amount of montmorillonite (Komine, 2008.). The hydraulic conductivity of three types of bentonites were unifiedly compared using the effective montmorillonite density obtained from Equations (3) and (4).

$$\rho_{em} = C_m \rho_d / \{100 - (100 - C_m)\rho_d/\rho_{nm}\} \tag{3}$$

$$\rho_{solid} = 100\rho_m / \{C_m + (100 - C_m)\rho_m/\rho_{nm}\} \tag{4}$$

where ρ_{em}: effective montmorillonite density, C_m: montmorillonite content, ρ_d: specimen dry density, ρ_{solid}: soil particle density of bentonite, ρ_{nm}: soil particle density of accessory minerals other than montmorillonite in bentonite, ρ_m: soil particle density of montmorillonite (= 2.77 Mg/m^3) (Lambe & Whitman. 1969).
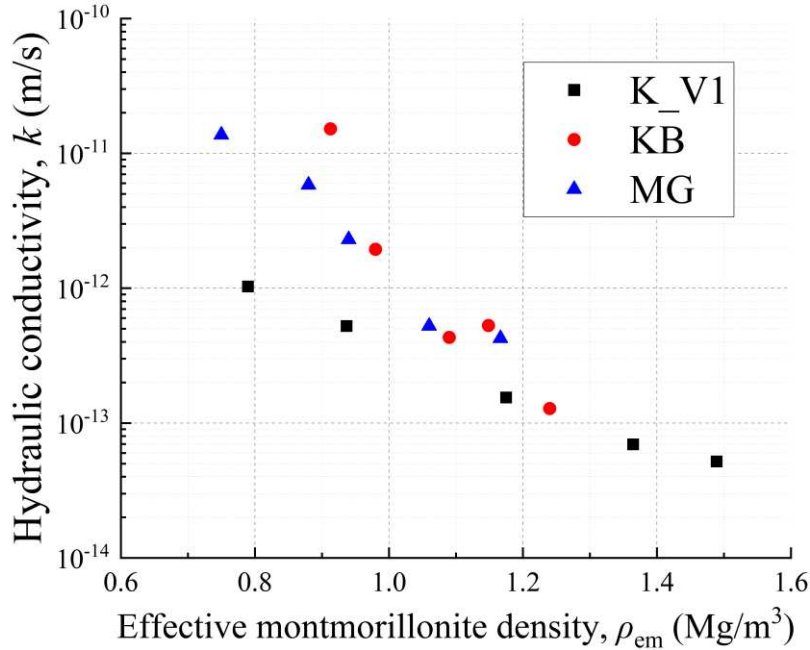
Figure 6. *Relation between hydraulic conductivity and effective montmorillonite density.*

Figure 6 shows the relationship between hydraulic conductivity and effective montmorillonite density. The k of MG and KB was 2 to 10 times higher than that of K_V1 in terms of ρ_{em} in the range of 0.8~1.2 Mg/m^3. Also, k of KB and MG were found to be almost the same under the same ρ_{em}. These results indicate that the permeability of bentonite with more Na$^+$ as an exchangeable cation in montmorillonite is lower than that of bentonite with more Ca^{2+} or Mg^{2+}. The results also suggest that Mg^{2+} ions as exchangeable cations in montmorillonite might have a similar effect on the hydraulic conductivity of bentonite as Ca^{2+} ions, which are also divalent cation.

Next, to consider the influence of Na$^+$, Ca^{2+} and Mg^{2+} ions on hydraulic conductivity as exchangeable cations, we also compare the calculation results of the theoretical equation for hydraulic conductivity (Komine, 2008.). Equations of (5)~(11) are the proposed equations for obtaining the hydraulic conductivity in Komine, 2008. In this calculation, R, which is a parameter on the ratio of density and coefficient of viscosity between interlayer water and free water, needs to be set. Based on the previous literature (Sato, 1971; Sato & Murota, 1971.), R values of 14 and 79 were adopted.

$$\varepsilon_{sv}^* = \{e_0 + \varepsilon_{s\,max}(e_0 + 1)/100\}\{1 + (100/C_m - 1)\rho_m/\rho_{nm} + (100/\alpha - 1)100/C_m \\ \cdot \rho_m/\rho_{sand}\}100 \tag{5}$$

$$e_0 = \rho_{solid}/\rho_{d0} - 1 \tag{6}$$

$$\rho_{solid} = (100/C_m \cdot 100/\alpha \cdot \rho_m)/\{1 + (100/C_m - 1)\rho_m/\rho_{nm} + (100/\alpha - 1)100/C_m \cdot \rho_m/\rho_{sand}\} \tag{7}$$

$$d_i = \varepsilon_{sv}^*/100(t + (R_{ion})_i) + (R_{ion})_i \tag{8}$$

$$k_i = \rho_{aw}/12\mu_{aw}(2d_i)^2 \tag{9}$$

$$\rho_{aw}/\mu_{aw} = 1/R \cdot \rho_{fw}/\mu_{fw} \tag{10}$$

$$k = 1/CEC \sum_{\substack{i=Na^+,Ca^{2+}, \\ K^+,Mg^{2+}}} [EXC_i k_i] \tag{11}$$

where, ε^*_{sv}: swelling volumetric strain of montmorillonite, $\varepsilon_{s\ max}$: maximum swelling strain of buffer and backfill materials, e_0: void ration of the materials, C_m: content of montmorillonite in the bentonite by percentage mass, ρ_{d0}: dry density of the materials, α: bentonite content in the materials by percentage mass, ρ_m: particle density of montmorillonite, ρ_{nm}: particle density of component minerals excluding montmorillonite in the bentonite, ρ_{sand}: particle density of sand in the materials, d_i: half the distance between two montmorillonite layers at the exchangeable cation which is either of Na+, Ca2+, K+ and Mg2+), k_i: hydraulic conductivity of two montmorillonite parallel-plate layers at the each exchangeable cation, ρ_{aw}: density of interlayer water between montmorillonite mineral layers, μ_{aw}: coefficient of viscosity of interlayer water between montmorillonite layers, $(R_{ion})_i$: non-hydrated radius of the exchangeable cation, ρ_{fw}: density of free water, μ_{fw}: coefficient of viscosity of free water, k : hydraulic conductivity of bentonite-based buffer and backfill materials, EXC_i: exchange capacity of the each exchangeable cation, and CEC: cation exchange capacity of bentonite.
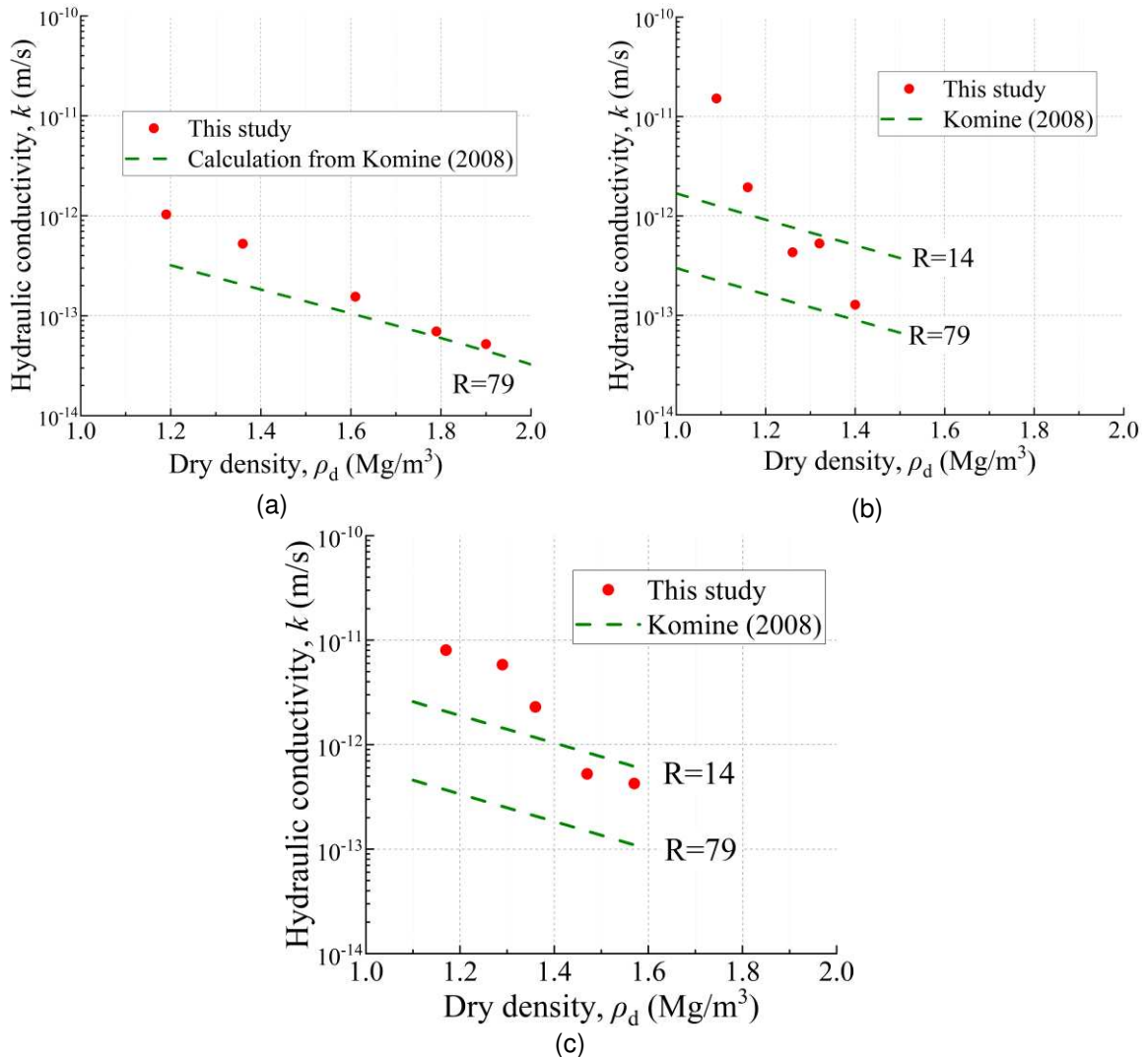
Figure 7. *Comparison between k value in this study and calculation result based on Komine (2008), (a) K_V1, (b) KB, and (c) MG.*

Figure 7 shows comparison between test results and calculation results. These results indicate that the Na-type bentonite K_V1 shows good agreement with the results in this study and calculation result of R=79. For the Ca-bentonite KB, and the Mg-Ca-bentonite MG, the measured values are higher than those for R=14 and R=79 at low dry density. One reason is for this that water flow in the specimen is assumed to be entirely between montmorillonite layers. At low dry density, it is possible that the Ca- or Mg-Ca-bentonite, which has lower swelling deformation property than Na-bentonite, may remain non-filling gaps outside the montmorillonite interlayer. Another reason is that the R value may be different from the actual one. In bentonite with high Ca^{2+} and Mg^{2+} ions, the diffused double layer in the montmorillonite interlayer is thinner than Na^+ ions, which may result in lower viscosity of the interlayer water at low dry density. However, as the dry density increases, the measured values are between the calculated values of R=14 and R=79, and the viscosity of the interlayer water has become closer to the assumed value in the calculation due to the reduction in the interlayer distance caused by compaction. Future studies should construct calculation method that can evaluate both water flow between montmorillonite layers and in the extra-laminar pore space and measure the viscosity of montmorillonite interlayer water to improve the accuracy of predictions. However, it is not realistic to use the low dry density range such as smaller than 1.4 Mg/m^3. In the relatively high dry density range of 1.4 Mg/m^3 or higher, the difference between test results and calculation result is within one order of magnitude, indicating that the prediction accuracy is higher for the dry density conditions considered to be used in actual radioactive waste disposals.

4   CONCLUSIONS

In this paper, three types of bentonites whose dominant exchangeable cation is different were used. The exchangeable cation effect on hydraulic conductivity was discussed by the test results using a newly developed hydraulic conductivity test system with a 2-mm-thick specimen. The results showed that k of all bentonites tended to decrease as dry density increased. The k of MG and KB was 2 to 10 times higher than that of K_V1 in terms of ρ_{em} in the range of 0.8~1.2 Mg/m^3. The k of KB and MG were found to be almost the same under the same ρ_{em}. Comparison of the calculated hydraulic conductivity by the theoretical evaluation and the measured hydraulic conductivity showed good agreement for K_V1 with high Na^+ content, while KB and MG with high divalent cations such as Ca^{2+} and Mg^{2+} resulted in a hydraulic conductivity estimate more than one order of magnitude lower in the low dry density. The reason for this may be that the viscosity of water between montmorillonite layers is set at a different value from the actual one.
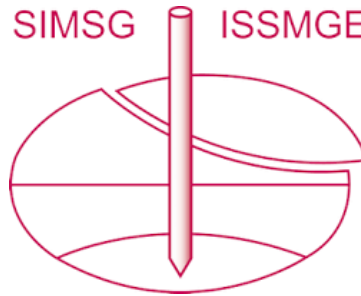
5   ACKNOWLEDGEMENTS

REFERENCES

Butsuda, R., Komine, H., Yasuhara, K., & Murakami, S. (2006). Advancement of experimentation for measuring hydraulic conductivity of bentonite using high-pressure consolidation test apparatus. Journal of Japan Society of Civil Engineers. Vol. 62. No. 3. pp.573-578.

Hasegawa, T. (2004). Investigation on the effect of seawater to hydraulic property and wetting process of bentonite. CRIEPI (Central Research Institute of Electric Power Industry) research report, N04005, Abiko, Japan.

Ito, D., Wang, H., & Komine, H. (2022). Hydraulic conductivity test system for compacted, 2-mm-thick bentonite specimens. Soils and Foundations. Vol. 62. No. 5. 101210. https://doi.org/10.1016/j.sandf.2022.101210

Japan Geotechnical Society (JGS). (2018). Test methods for permeability of low-permeable saturated soils. JGS0312-2018.

Kobayashi, I., Owada, H., Ishii, T. and Iizuka, A. (2017). Evaluation of specific surface area of bentonite-engineered barriers for Kozeny–Carman law. Soils and Foundations. Vol. 57. pp. 683-697.

Komine, H. (2008). Theoretical equations on hydraulic conductivities of bentonite-based buffer and backfill for underground disposal of radioactive wastes. Journal of Geotechnical and Geoenvironmental Engineering. Vol. 134. No. 4. pp.497-508.

Komine, H., & Ogata, N. (1994). Experimental study on swelling characteristics of compacted bentonite. Canadian Geotechnical Journal. Vol. 31. No. 4. pp.478-490.

Lambe, T.W. & Whitman, R.V. (1969). Soil Mechanics. John Wiley & Sons Inc. pp.29-31.

Matsumoto, K., Sugano, T., Fujita, T., & Suzuki, H. (1997). Permeability of saturated bentonite buffer material. Report of Power Reactor and Nuclear Fuel Development Corporation. PNC TN8410 97-296.

Nishimura, T., Koseki, J., Fredlund, D. G., & Rahardjo, H. (2011). Microporous membrane technology for measurement of soil-water characteristics curve. Geotechnical Testing Journal. Vol. 35. No. 1. pp.1-8.

Nuclear Waste Management Organization of Japan (NUMO) (2022). Fundamental Engineering Properties of Compacted Japanese Bentonites and Bentonite-Sand Mixtures. NUMO-TR-21-02. pp. 61-66.

Pusch, R., 1992. Use of bentonite for isolation of radioactive waste products. Clay Minerals, 27, 353-361.

Sato, K. (1971). On an effect of absorbing water for micro-seepage. *Journal of Japan Society of Civil Engeers.* Vol. 187. pp.67–77.

Sato, K., & Murota, A. (1971). Experimental study on the absorbed water for micro-seepage. *Journal of Japan Society of Civil Engeers.* Vol. 195. pp. 67–75.

Sellin, P., Leupin, O. X., 2013. The use of clay as an engineered barrier in radioactive-waste management－A review. Clays and Clay Minerals, 61(6), 477-498.

Shirakawabe, T., Wang, H., Morodome, S., & Komine, H. (2022). On methods to measure cation exchange capacity and amounts of leached cations of bentonites. Japanese Geotechnical Journal. Vol. 17. No. 1. pp.61-71.

Wang, H., Ito, D., Shirakawabe, T., Ruan, K., & Komine, H. (2022a). On swelling behaviours of a bentonite under different water contents. Géotechnique. https://doi.org/10.1680/jgeot.21.00312

Wang, H., Ruan, K., Harasaki, S., & Komine, H. (2022b). Effects of specimen thickness on apparent swelling pressure evolution of compacted bentonite. Soils and Foundations. Vol. 62. No. 1. https://doi.org/10.1016/j.sandf.2021.101099

INTERNATIONAL SOCIETY FOR SOIL MECHANICS AND GEOTECHNICAL ENGINEERING

The paper was published in the proceedings of the 9th International Congress on Environmental Geotechnics (9ICEG), Volume 3, and was edited by Tugce Baser, Arvin Farid, Xunchang Fei and Dimitrios Zekkos. The conference was held from June 25th to June 28th 2023 in Chania, Crete, Greece.